

Supplemental Methods

Cell culture. Human RPE1 cells were acquired from the American Type Culture Collection. RPE1 cells were cultured in DMEM/F12 (Welgene) supplemented with 10% FBS (Welgene) and penicillin/streptomycin (Welgene). Ciliogenesis in RPE1 cells was induced by serum starvation (0% FBS) for 24 h or 48 h.

Plasmids, transfection, and cell line establishment. RPE1-Smo-EGFP cells were established as previously reported (13). Plasmids were acquired from Addgene: pmCherry-CEP290 (#27380), pSpCas9(BB)-2A-Puro (#62988), pLKO.1-TRC (#10878). pSpCas9(BB)-2A-Puro vector expressing sgRNA specific for *CEP290* Exon 2 (pSpCas9(BB)-2A-Puro-CEP290) was constructed according to a published protocol (10). pLKO.1 vectors expressing control and NPHP5 shRNA were constructed according to Addgene's protocol. Plasmid transfection was performed using Lipofectamine LTX and PLUS reagent (Invitrogen) according to the manufacturer's forward transfection protocol. To establish a CEP290^{null} RPE1-Smo-EGFP cell line, RPE1-Smo-EGFP cells were transfected with pSpCas9(BB)-2A-Puro-CEP290, and selected with 12 µg/mL puromycin for 3 days. Subsequently, a single colony harboring frameshift mutations on both copies of the *CEP290* gene was selected for further study. Sequences of shRNA, sgRNA, and sequencing primers are provided in the Supplemental Table 2.

Compound library screening. A custom library composed of FDA-approved drugs (Johns Hopkins Drug Library) and natural compounds was screened (total 2,789 compounds). CEP290^{null} RPE1-Smo-EGFP cells were seeded on black, clear-bottomed 96-well plates (Falcon #353219) at 2.5×10^4 cells per well. After 24 h incubation, cells were serum-starved, and compounds from library stock plates [1 mM stock in dimethylsulphoxide (DMSO)] were treated at a final concentration of 10 µM. Cells were fixed with 4% paraformaldehyde for 8 min after 48 h

compound treatment. Image acquisition was performed using a DeltaVision Spectris Imaging System. Primary cilia were identified by Smo-EGFP fluorescence. The image analysis algorithm that was used in the previous RNAi screening for ciliogenesis regulators (13) did not reliably identify ciliary Smo-EGFP fluorescence in CEP290^{null} RPE1-Smo-EGFP cells. Thus, the number of ciliated cells was counted manually.

siRNA and reagents. siRNA transfection was performed using Lipofectamine RNAiMAX (Invitrogen) according to the manufacturer's reverse transfection protocol. Cells were fixed 48-72 h after siRNA transfection. AllStars Negative Control siRNA (Qiagen) was used as a control siRNA. The sequence of siRNAs used in this study is provided in the Supplemental Table 2. CytoD (Sigma-Aldrich) was treated at 200 nM. Cells were treated with eupatilin (Adipogen; AG-CN2-0432) at 20 μ M unless otherwise indicated for 24 h or 48 h. Jaceosidin (CFN90386) and Lysionotin (CFN99787) were purchased from ChemFaces. MK-2206 2HCl (S1078) and BYL-719 (S2814) were purchased from Selleckchem. WY-14643 (C7081) and SAG (SML1314) were purchased from Sigma-Aldrich. Acepromazine and methdilazine in Johns Hopkins FDA-approved Drug Library were used at final concentration of 20 μ M.

Antibodies. The antibodies used for western blotting and immunofluorescence were as follows: anti-glutamylated Tubulin (1:750 for immunofluorescence; AG-20B-0020, Adipogen), anti-ARL13B (1:1000 for immunofluorescence; 17711-1-AP, Proteintech), Alexa Fluor 594 phalloidin (1:1000 for immunofluorescence; Thermofisher), Ki67 (1:500 for immunofluorescence; ab15580, Abcam), anti-YAP1 (1:500 for immunofluorescence; sc-101199, Santa Cruz), anti-NPHP5 (1:1000 for immunofluorescence, 1:500 for western blotting; HPA042028, Sigma-Aldrich), anti-NPHP5 (2.5 μ g for co-immunoprecipitation, 1:200 for western blotting; ab69927, Abcam), anti-calmodulin (1:1500 for western blotting; 05-173, Millipore), anti-TCTN1 (1:100 for

immunofluorescence; 15004-1-AP, Proteintech), anti-IFT88 (1:500 for immunofluorescence; 13967-1-AP, Proteintech), anti-IFT88 (1:500 for western blotting; 60227-1-Ig, Proteintech), anti-opsin (1:200 for immunofluorescence; AB5404, Sigma-Aldrich), anti-rhodopsin (1:500 for immunofluorescence; MAB5316, Chemicon), anti-TTBK2 (1:300 for immunofluorescence; 15072-1-AP, Proteintech), anti-beta-catenin (1:1000 for western blotting; ab6302, Abcam), and anti-CP110 (1:250 for immunofluorescence; 12780-1-AP, Proteintech). Anti-TMEM216 antibody was provided by Jeong Ho Lee (Graduate School of Medical Science and Engineering, KAIST, Daejeon, Korea).

Immunofluorescence. For indirect immunofluorescence, cells were grown in 8-well Lab-Teck II chamber slides (Nunc) or 96-well plates (BD Falcon). Cold methanol (for 5 min) or 4% paraformaldehyde (for 8 min) was used for fixation. When cells were fixed with 4% paraformaldehyde, they were permeabilized using 0.1% Triton-X-100 (Sigma-Aldrich). After blocking with 5% FBS for 10 min, cells were incubated with primary antibodies at RT for 30 min or 1 h, or at 4°C overnight. Thereafter, cells were incubated with Alexa Fluor 488-, 594-, or 647-conjugated secondary antibody (ThermoFisher) at RT for 30 min or 1 h. Alexa Fluor 594-phalloidin was used for filamentous actin staining. Cells were mounted with mounting solution (75% glycerol, 20 nM Tris, and 0.02% NaN₃) containing 0.5 µg/mL 4, 6,-diamidino-2-phenylindole (DAPI, Sigma-Aldrich) for fluorescence microscopic imaging.

Fluorescence microscopy. DeltaVision Spectris Imaging System (Applied Precision) equipped with an Olympus IX70 inverted microscope was used for immunofluorescence image acquisition. Details of imaging were previously described (12, 14). Acquired images were processed and analyzed using ImageJ software (NIH) and Adobe Photoshop CS6 (Adobe System).

Cell proliferation assay. RPE1 cells were seeded on clear-bottomed 96-well plates at 150

cells per well. Twenty-four hours later, cytoD or eupatilin was added to the plates at the indicated concentrations. Cells were further incubated for 96 h, and viable cells were quantified using Cell Counting Kit-8 (Dojindo) according to the manufacturer's instructions.

Mice and treatment. Specific pathogen-free *rd16*^{homo} mice were acquired from the Jackson Laboratory (#000031). CD-1 and C57BL/6N mice were purchased from ORIENT BIO. Mice were transferred, established, and bred in an animal facility at KAIST and fed with free access to standard diet (PMI LabDiet) and water. *Rd16*^{het} mice were generated by crossing *Rd16*^{homo} mice with C57BL/6N mice. *Rd16*^{het} and *Rd16*^{homo} mouse neonates (n = 3 mice for each group), and CD-1 mouse neonates (n = 8 mice for each group) were subcutaneously injected with 40 mg/kg of eupatilin dissolved in DMSO/PBS (v/v 3%) daily from postnatal day 3. Periocular injection (n = 3 mice for each group) was done with 0.015 mg of eupatilin dissolved in DMSO/PBS (v/v 10%) under topical anesthesia (0.5% proparacaine hydrochloride eye drop; Alcon). Retinas were harvested at postnatal day 23 or 30.

Electroretinography. Retinal functions were evaluated using electroretinography at postnatal day 23 or 30. Before recording photopic and scotopic responses, mice were light- or dark-adapted for 12 h, respectively. Pupils were dilated using 1% tropicamide and 2.5% phenylephrine eye drops (Santen Pharmaceutical). After anesthesia (i.p. ketamine 40 mg/kg and xylazine 5mg/kg), a gold-plated objective lens was placed on the cornea, and silver-embedded needle electrodes were placed at the forehead (reference) and tail (ground). The electroretinographic stimulus and recording were performed using LabScribe ERG equipped with a retinal imaging microscope (Phoenix Research Labs, Micron IV) following the manufacturer's instructions. To measure scotopic responses, a digital bandpass filter ranging from 0.5 to 1000 Hz and a stimulus of 2.2 log (cd·s/m²) were used. A filter ranging from 2 to 200 Hz and a stimulus of

2.2 log (cd·s/m²) with a 1.3 log (cd·s/m²) background were used to obtain photopic b-waves. After signal averaging, the amplitudes of the a- and b-waves were obtained and analyzed using LabScribe ERG version 3 software.

Western blotting. For western blot analysis, cells were lysed on ice in RIPA lysis buffer (20 mM HEPES, 150 mM NaCl, 1% NP-40, 0.25% sodium deoxycholate, and 10% glycerol) supplemented with protease and phosphatase inhibitors (Merck Millipore). Cell lysates were sonicated with a Branson Digital Sonifier 250 (Branson Ultrasonics) and then subjected to centrifugation (18,000 g) at 4°C for 10 min. Protein concentration of the supernatants was measured using a BCA protein assay kit (PIERCE). Aliquots of each protein lysate (10–20 µg) were used for SDS-polyacrylamide gel electrophoresis. Proteins were transferred to nitrocellulose membranes and incubated for 45 min with blocking solution (TBST buffer with 5% skim milk). Blocked membranes were incubated with primary antibody at 4°C overnight, and then incubated with secondary antibody (Abcam) at 4°C for 1 h. Proteins were detected using enhanced chemiluminescence western blot detection solution (WesternBright, Advansta).

Drug affinity responsive target stability (DARTS) assay. DARTS assay was conducted according to a published protocol (28). Subconfluent cells in a 100 mm culture dish were lysed with 1 mL of NP-40 lysis buffer. Lysates were incubated on ice for 10 min and then centrifuged at 18,000 g for 10 min at 4°C. BCA assay was performed to determine protein concentration of the cell lysates. Cell lysate were divided into two aliquots and treated with DMSO (0.1%) or eupatilin (100 µM). After incubation with DMSO or eupatilin at RT for 15 min in a thermomixer, pronase (Roche) was added at 0, 62.5 ng, 250 ng, or 1 µg per 100 µg total cell protein. Lysate-pronase mixtures were incubated at RT for 15 min, and then protease inhibitor cocktail was added to stop

digestion. For each treatment, 10 μ g of protein lysate was applied to SDS-polyacrylamide gel electrophoresis for western blotting.

Co-immunoprecipitation. Subconfluent cells were cultured in serum-free DMEM/F12 with 50 μ M eupatilin or 0.05% DMSO for 48 h. Cells were washed with cold PBS and lysed with cooled 1 mL NP-40 buffer. Cell lysates were passed through a cooled syringe with a 26-gauge needle and incubated on ice for 10 min. Cell lysates were incubated with Protein G agarose beads (Pierce #22851) for pre-clearing. After removing Protein G agarose beads, lysates were incubated with anti-NPHP5 antibody (2.5 μ g) at 4 $^{\circ}$ C overnight. Lysate-antibody mixtures were incubated with Protein G agarose beads at 4 $^{\circ}$ C for 2 h. Beads were washed four times with NP-40 lysis buffer. Pellets were resuspended with 2X SDS sample buffer and boiled for 5 min. Samples were applied to SDS-polyacrylamide gel electrophoresis for western blotting.

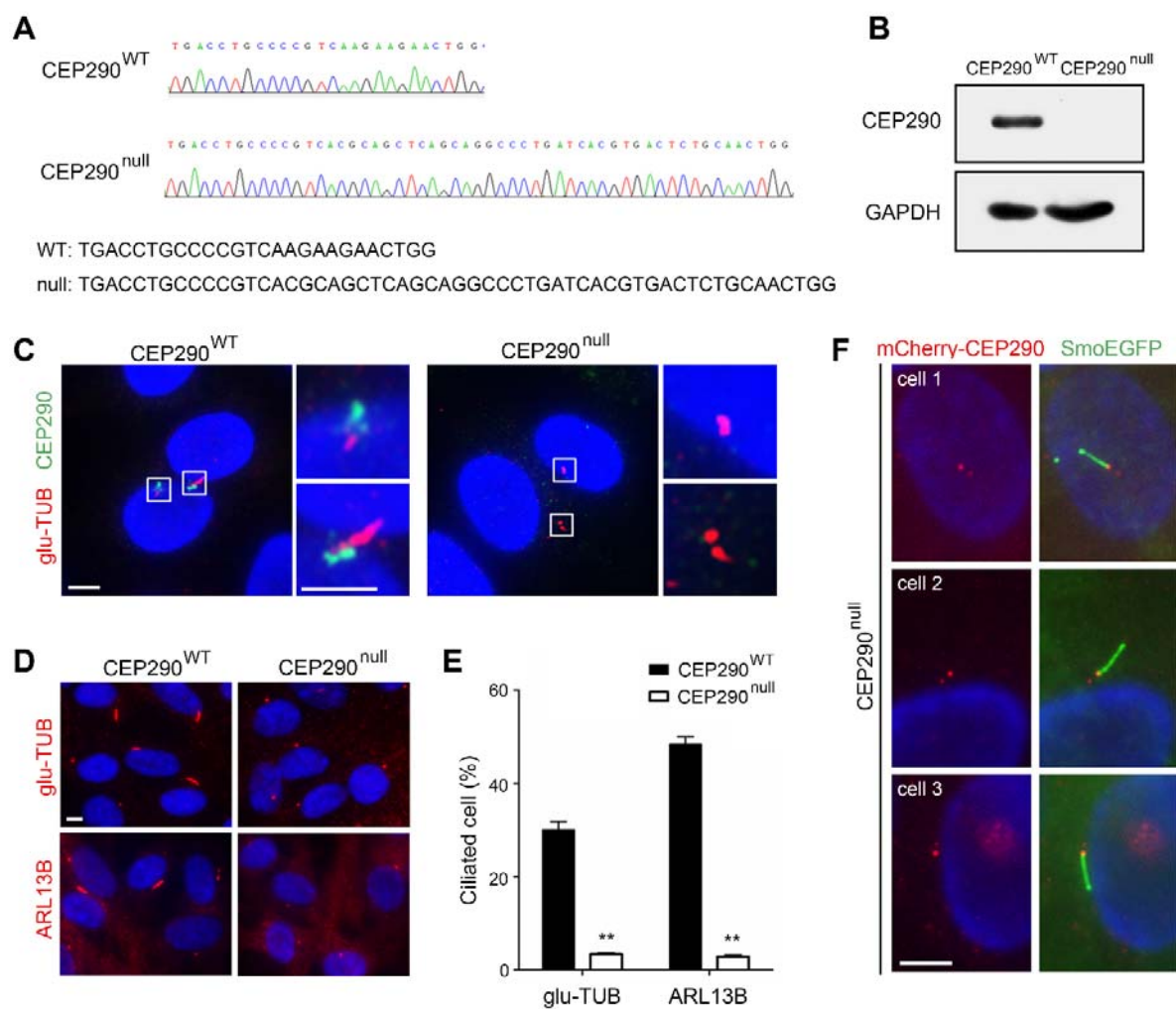
In silico docking simulation. All molecular docking analysis was performed with Discovery Studio 2016 software (Accelrys, Inc.) adopting the CHARMM force field. The crystal structure of human calmodulin (Protein Data Bank code 1CTR) was obtained from the RCSB protein data bank. The molecular structure of eupatilin (PubChem CID 5273755) was obtained from PubChem. Calmodulin and eupatilin were optimized by clean protein and ligand prepare respectively. To dock the ligands, CDOCKER docking method was performed. The parameters and binding site of CDOCKER were validated using a eupatilin from RSCB protein data bank of the calmodulin crystal structure. All molecules were docked to the binding site of the protein and top hit 10 poses were generated (Pose Cluster Radius 0.5, Radius size of site sphere from Sphere Object Attributes 10.3 \AA). The binding energy (CDOCKER energy) were determined by calculating the binding energy of the most predictive binding mode.

Supplemental Table 1. List of compounds that increased the number of ciliated cells.

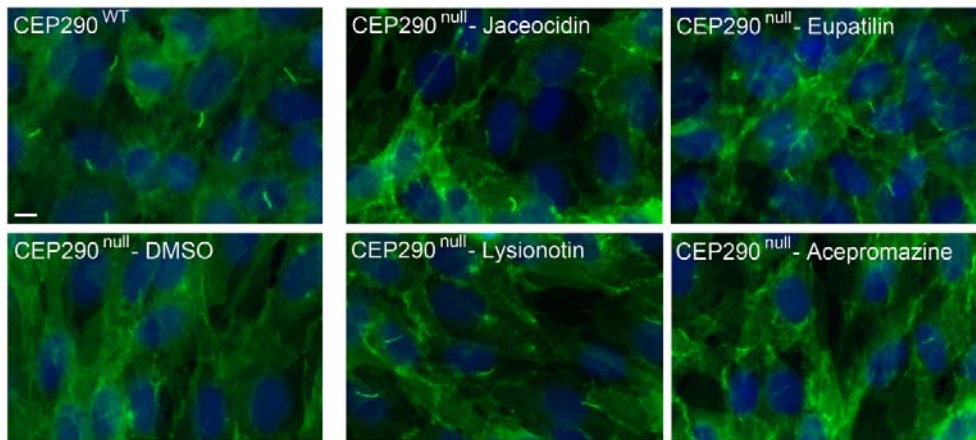
PubChem CID	Compound name	Ciliated cell (%)	Description
5379096	Jaceosidin	24.5	Flavonoid
160921	Lysionotin	24.2	Flavonoid
5273755	Eupatilin	24.2	Flavonoid
6077	Acepromazine	22.6	Phenothiazine derivative psychotropic drug
14677	Methdilazine	22.3	Phenothiazine compound with antihistamine activity
5280343	Quercetin	21.8	Flavonoid
123618	Norastemizole	21.7	Anti-histamine (H1 antagonist)
27990	Vitamin E Nicotinate	19.4	Vitamine
9033	Aziridine	19.3	Monofunctional alkylating agent with potential antineoplastic activity
1057	Pyrogallol	18.9	Trihydroxybenzene
23663967	Bucladesine sodium	17.1	Cyclic nucleotide derivative that mimics the action of endogenous cyclic AMP
3058739	Safingol	17.0	Saturated derivative of sphingosine. Protein kinase C (PKC) inhibitor
1967	Docebenone (AA-861)	15.9	5-Lipoxygenase inhibitors
3474	Glafenine	14.1	Anthranilic acid derivative with analgesic properties
54676539	Meclocycline	11.7	Tetracycline antibiotic
5284373	Cyclosporin A	11.6	Calcineurin inhibitor immunosuppressant
2081	Alaproclate	11.5	Antidepressive agent, serotonin uptake inhibitor
9677	Nandrolone decanoate	11.0	Synthetic androgen and anabolic steroid
3308	Etodolac	10.6	Nonsteroidal anti-inflammatory agent with potent analgesic and antiarthritic properties
460	Guaiacol	10.5	Phenolic compound with disinfectant properties
2202	Anthralin	10.5	Anthraquinone derivative with anti-psoriatic and anti-inflammatory properties
6114	Methacholine chloride	10.4	Quaternary ammonium parasympathomimetic agent with the muscarinic actions of acetylcholine

Supplemental Table 2. sgRNA, primer, shRNA, and siRNA sequences.

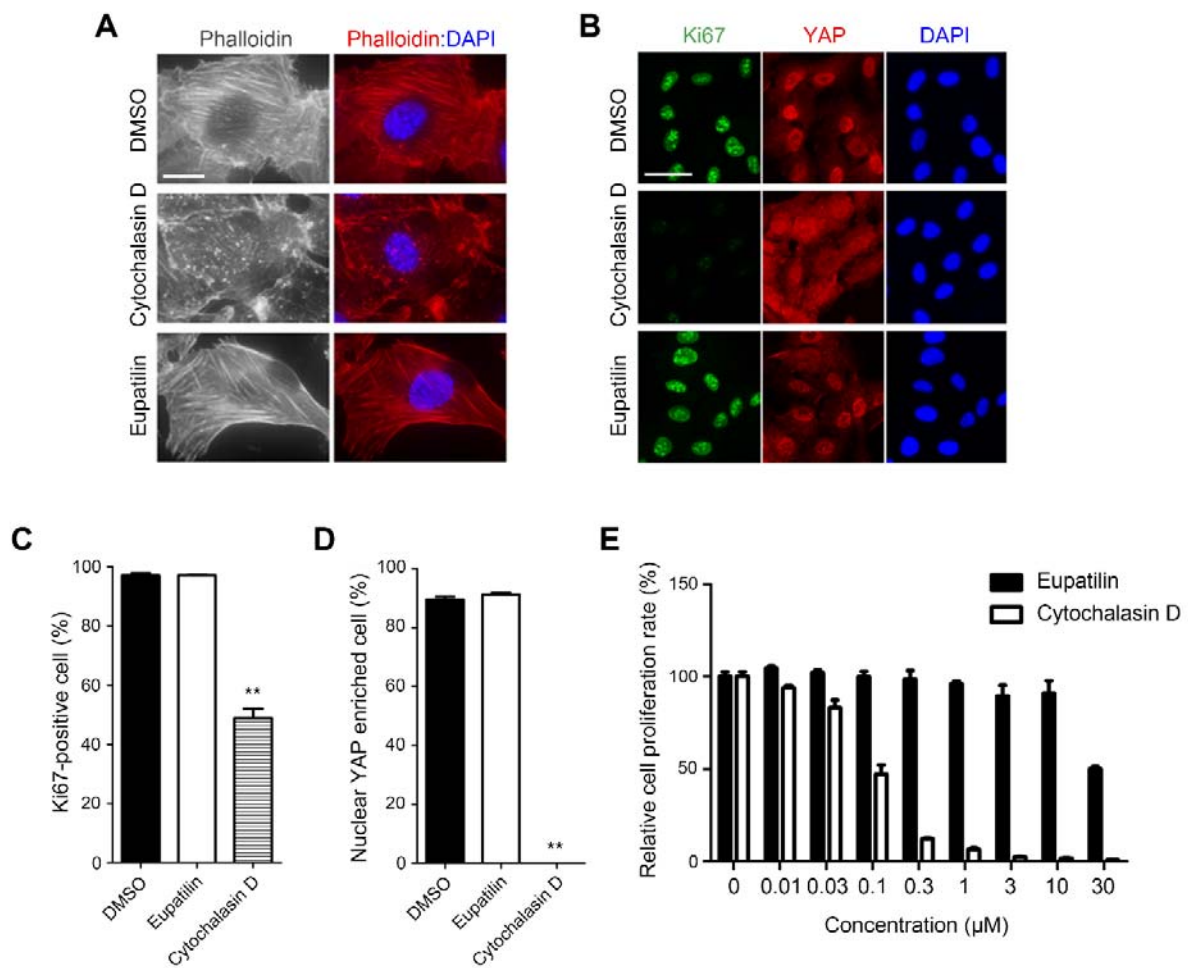
CRISPR-Cas9		
sgRNA targeting CEP290 Exon 2		CCTGCCCCGTCAAGAAGAAC
Exon2 sequencing primers	Forward	CCACTTGTCTATTTTGTGGCC
	Reverse	CTTCCACCTAAGTAAACAGAAAAGC
shRNA sequence		
Control		CCTAAGGTTAAGTCGCCCTCG (addgene #1864)
NPHP5		(AA)CAGTCTCTCATAGAGTATA (Dharmacon V2LHS_79720)
siRNA sequence		
Control		Allstars negative control siRNA (Qiagen)
CEP164		GAGUGAAGGUGUAUCGCUU
CEP83	#1	AGGUGAAGUUGGUGACUCA
	#2	GGAACUAGUUAGAGUCAAG
C5ORF42	#1	CAUCAUCAGUACUGGUUAA
	#2	GAAUCAAAACCUAAGAGGAU
	#3	AUGAUAAGGUGGUCUAAUA
	#4	UAACAAACUUGGUUGGACA
TTBK2	#1	GACCAUGUUUGUAGAUUUU
	#2	UGGCUUGGCUCGACAAUUU
	#3	GGGCAGCAUUGUAUUGAGA
	#4	GACCAUAUCUCUUCUUUGG
NPHP4	#1	AAGCAACGAGAUGGUGCUACA
	#2	CAGAUCUCGGGUCAUCUCAA
MKS1	#1	GAAAUUACGAUCGACAAU
	#2	CCUCGUAGGCACCGACUUU
	#3	GGCGAGUGUUCAAGGAUCU
	#4	ACACUGACUCUGAUAGUA
CALM1	#1	CAAGUCAACUAUGAAGAAU
	#2	GAAGCUGAAUUGCAGGAUA
CALM2	#1	GUUAAACAGAUGAAGAAGUU
	#2	UAACAACAAAGGAAUUGGG
CALM3	#1	GAGAUGGCCAGGUCAAUUA
	#2	GGAUGGAGAUGGCACUAUC



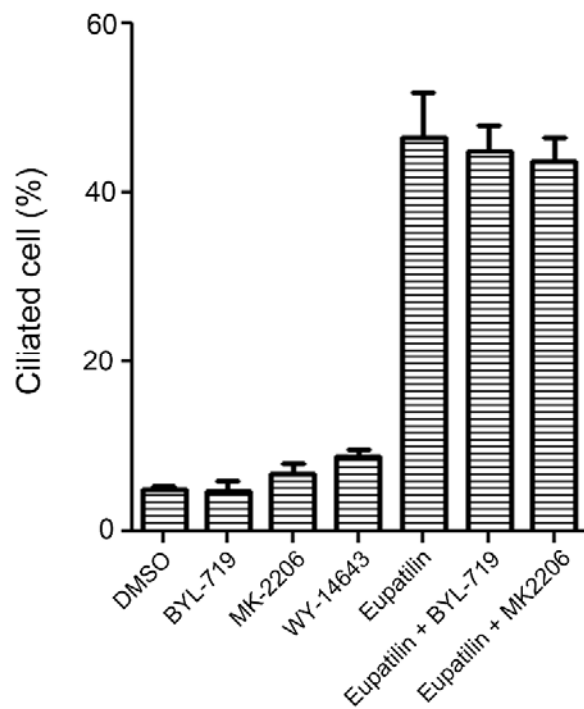
Supplemental Figure 1. Establishment and characterization of CEP290^{null} RPE1-Smo-EGFP cells. (A) Sequence of the homozygous *CEP290*^{null} allele generated by the CRISPR-Cas9 system. (B) Western blot analysis demonstrating the loss of CEP290 in CEP290^{null} RPE1-Smo-EGFP cells. (C) Immunofluorescence micrographs confirming the loss of CEP290 in CEP290^{null} RPE1-Smo-EGFP cells. (D) Defective ciliogenesis in CEP290^{null} RPE1-Smo-EGFP cells. Ciliogenesis was induced by serum starvation for 48 h. Anti-glutamylated Tubulin (glu-TUB) and anti-ARL13B antibodies were used as cilium markers. (E) Quantification of the experiment shown in (D). (F) Rescue of defective ciliogenesis in CEP290^{null} RPE1-Smo-EGFP cells using transient expression of mCherry-tagged CEP290. Nuclei were marked with DAPI (blue). Scale bars indicate 5 μ m. Error bars represent SEM (n = 3 independent experiments; **P < 0.01, t-test).



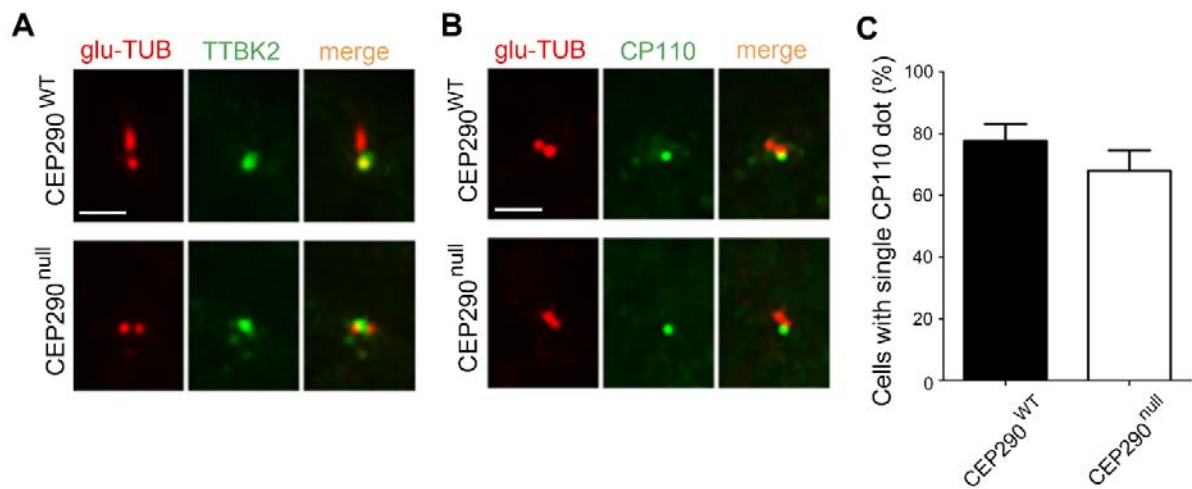
Supplemental Figure 2. Fluorescence micrographs of control and screen hits. Rescue of defective ciliogenesis in CEP290^{null} RPE1-Smo-EGFP cells. Indicated compounds were treated at a final concentration of 10 μ M. Smo-EGFP stably expressed in CEP290^{null} RPE1-Smo-EGFP cells was used as a cilium marker. Nuclei were marked with DAPI (blue). Scale bar indicates 5 μ m.



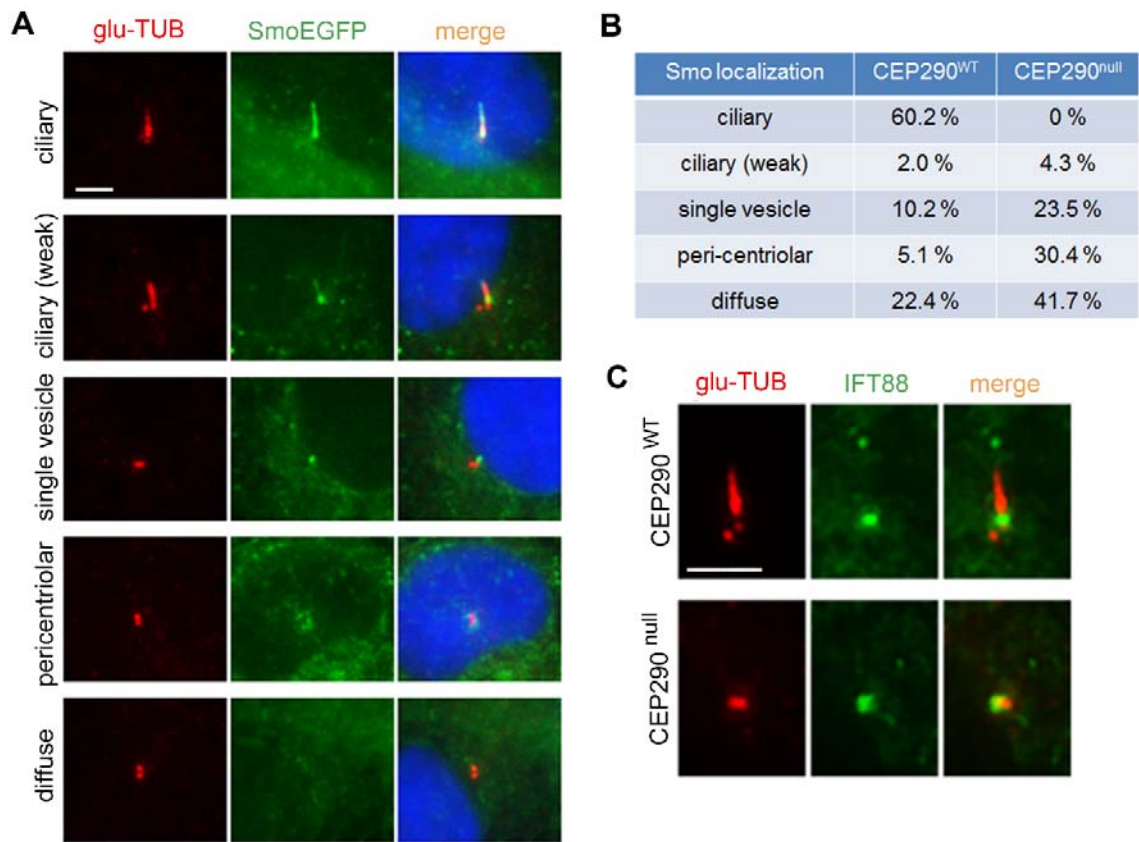
Supplemental Figure 3. Effect of cytochalasin D and eupatilin on the actin cytoskeleton and cell proliferation. (A) Fluorescence micrographs visualizing actin filaments stained with phalloidin-Alexa Fluor 594 after treatment with DMSO, cytoD (200 nM), or eupatilin (20 μM) for 3 h. (B) Immunofluorescence micrographs visualizing Ki67 expression and YAP1 subcellular localization in CEP290^{null} RPE1-Smo-EGFP cells after treatment with DMSO, cytoD, or eupatilin for 24 h. (C, D) Quantification of the experiment presented in (B). (E) Eupatilin and cytoD dose-responses of RPE1 cells. Nuclei were marked with DAPI (blue). Scale bars indicate 20 μm (A) and 40 μm (B). Error bars represent SEM (n = 3 independent experiments; **P < 0.01, t-test).



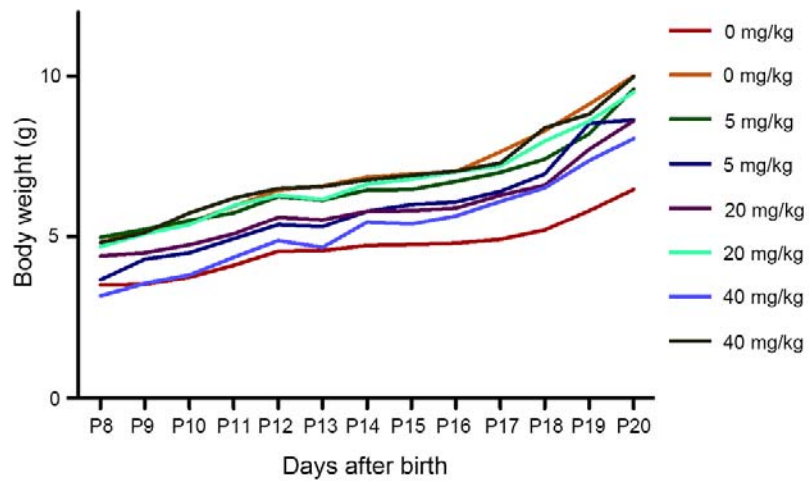
Supplemental Figure 4. Effect of PI3K and AKT inhibitors, PPAR- α agonist and eupatilin on ciliogenesis in CEP290^{null} RPE1-Smo-EGFP cells. BYL-719 (PI3K inhibitor, 50 nM), MK-2206 (AKT inhibitor, 10 μ M), and WY-14643 (PPAR- α agonist, 10 μ M) were treated alone or combined with eupatilin (20 μ M). Anti-ARL13B antibodies were used as a cilium marker. Error bars represent SEM (n = 3 independent experiments).



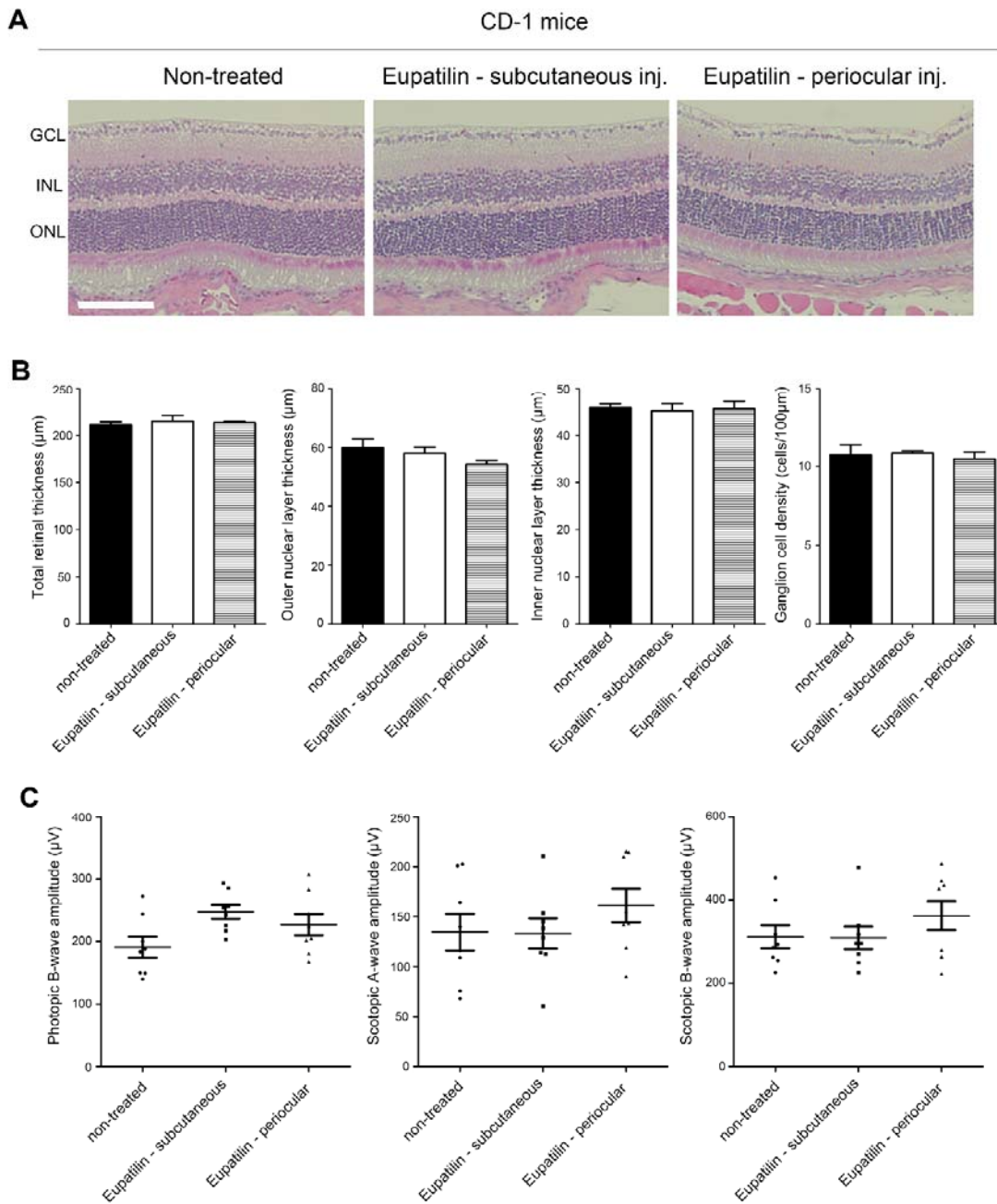
Supplemental Figure 5. TTBK2 centrosomal recruitment and CP110 cap removal in CEP290^{null} RPE1-Smo-EGFP cells. (A) Immunofluorescence micrographs visualizing TTBK2 at the centrosomal area in CEP290^{WT} and CEP290^{null} RPE1 cells after serum starvation for 16 h. Anti-glu-TUB antibody labels the centriole/basal body and the ciliary axoneme. (B) Immunofluorescence micrographs visualizing CP110 at the centrosomal area in CEP290^{WT} and CEP290^{null} RPE1 cells after serum starvation for 24 h. (C) Quantification of cells exhibiting single CP110 dot attached to the centriole. Scale bars indicate 5 μ m. Error bars represent SEM (n = 3 independent experiments).



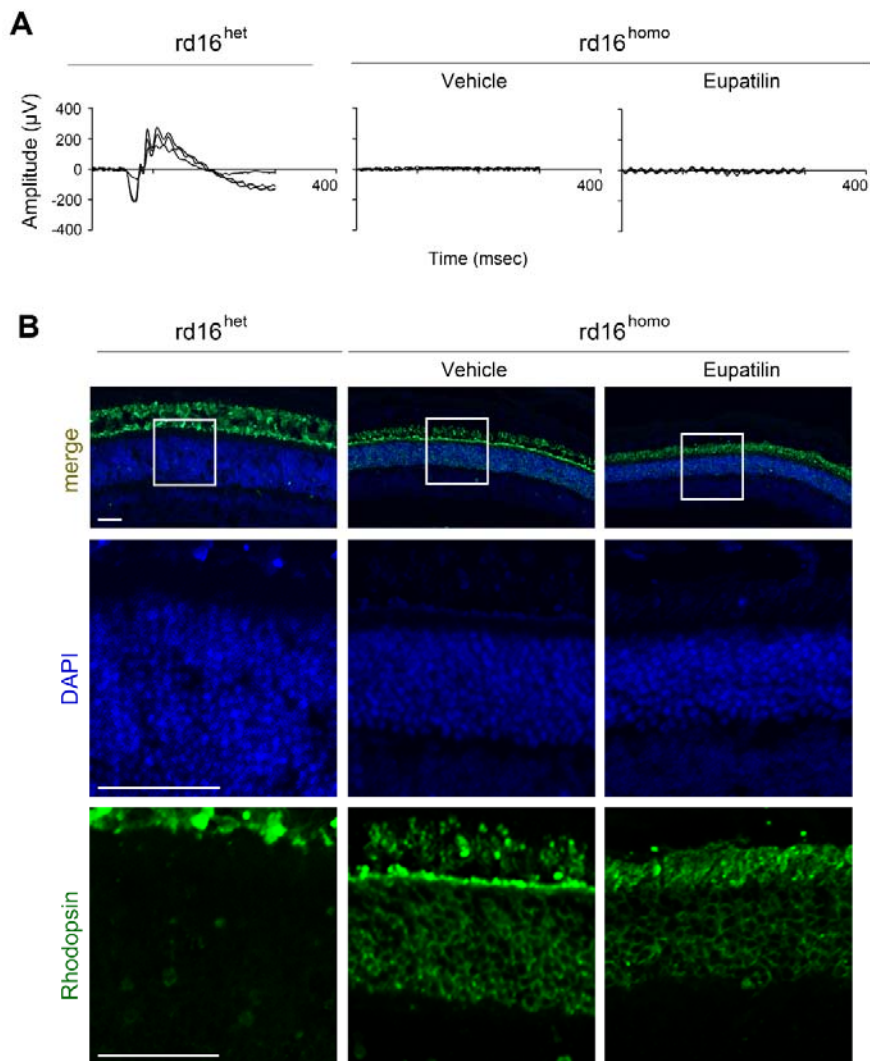
Supplemental Figure 6. Subcellular localization patterns of Smo-EGFP in CEP290^{WT} and CEP290^{null} RPE1 cells. (A) Fluorescence micrographs visualizing various patterns of Smo-EGFP localization at the centrosomal area in CEP290^{WT} and CEP290^{null} RPE1-Smo-EGFP cells after serum starvation for 24 h. The cilium and the centriole were identified by anti-glu-TUB antibody staining. (B) Quantification of the experiment presented in (A). (C) Immunofluorescence micrographs visualizing apparently normal centrosomal recruitment of IFT88 in CEP290^{null} RPE1-Smo-EGFP cells after serum starvation for 24 h. Nuclei were marked with DAPI (blue). Scale bars indicate 5 μ m.



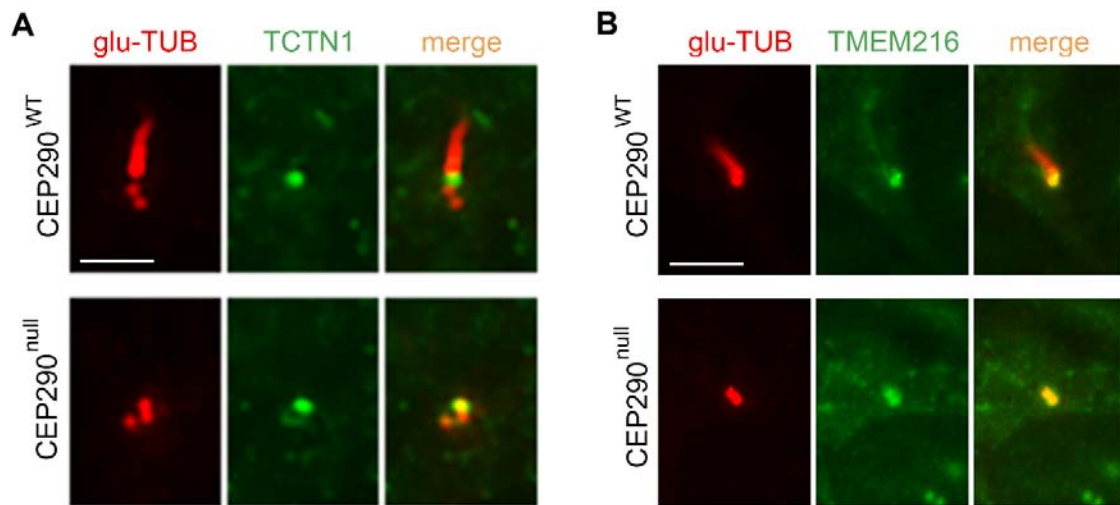
Supplemental Figure 7. Effect of eupatilin injection on the survival and growth of CD-1 mouse neonates. Eupatilin (0 to 40 mg/kg) was subcutaneously injected daily into the neck of CD-1 neonates from postnatal day 3. Body weight was measured from postnatal day 8.



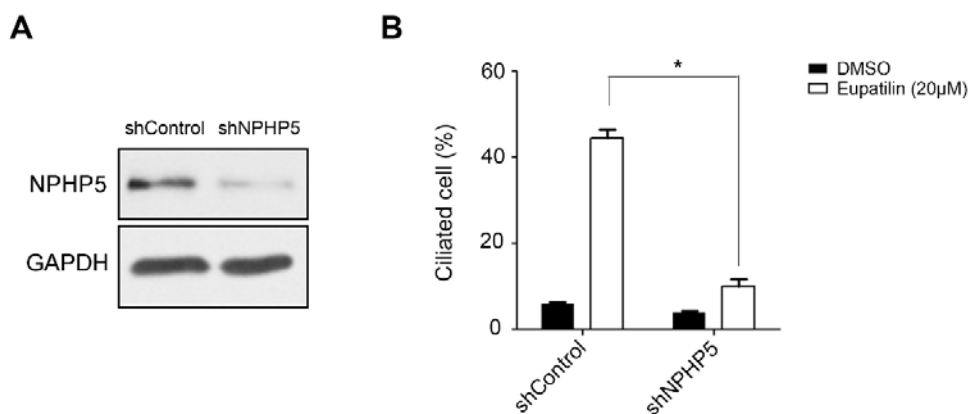
Supplemental Figure 8. Effect of eupatilin on the structure and electrophysiological function of the retina. (A) Hematoxylin-eosin staining of retina after daily injection of eupatilin for 4 weeks from postnatal day 3. (B) Quantification of the experiment presented in (A). (C) Amplitude of A- and B-wave in photopic or scotopic electroretinograms. Scale bar indicates 100 μm. Error bars represent SEM (A, B, n = 4 mice, each group; C, n = 8 mice, each group).



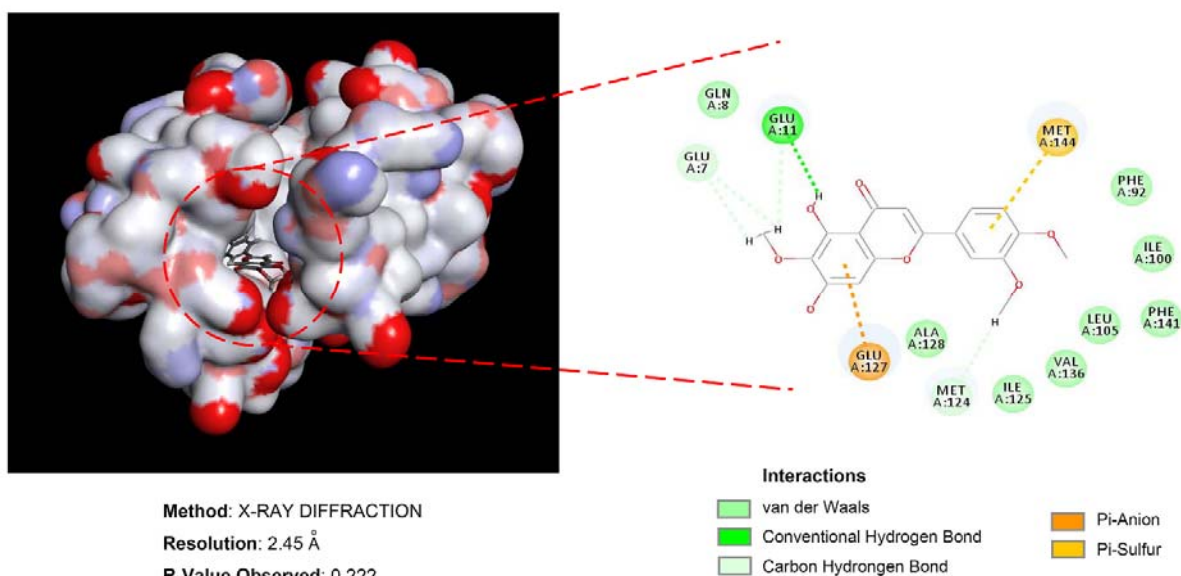
Supplemental Figure 9. Eupatilin injection does not rescue rhodopsin trafficking defects in *rd16*^{homo} retinas. (A) Electroretinograms of *rd16*^{het} and *rd16*^{homo} mice under dark adapted condition after daily injection of vehicle or eupatilin (40 mg/kg) for three weeks from postnatal day 3 (n = 3 mice, each group). (B) Immunofluorescence micrographs visualizing rhodopsin in the retina of *rd16*^{het} and *rd16*^{homo} mice injected with vehicle or eupatilin (40 mg/kg) for three weeks from postnatal day 3. Nuclei were marked with DAPI (blue). Scale bars indicate 25 μm.



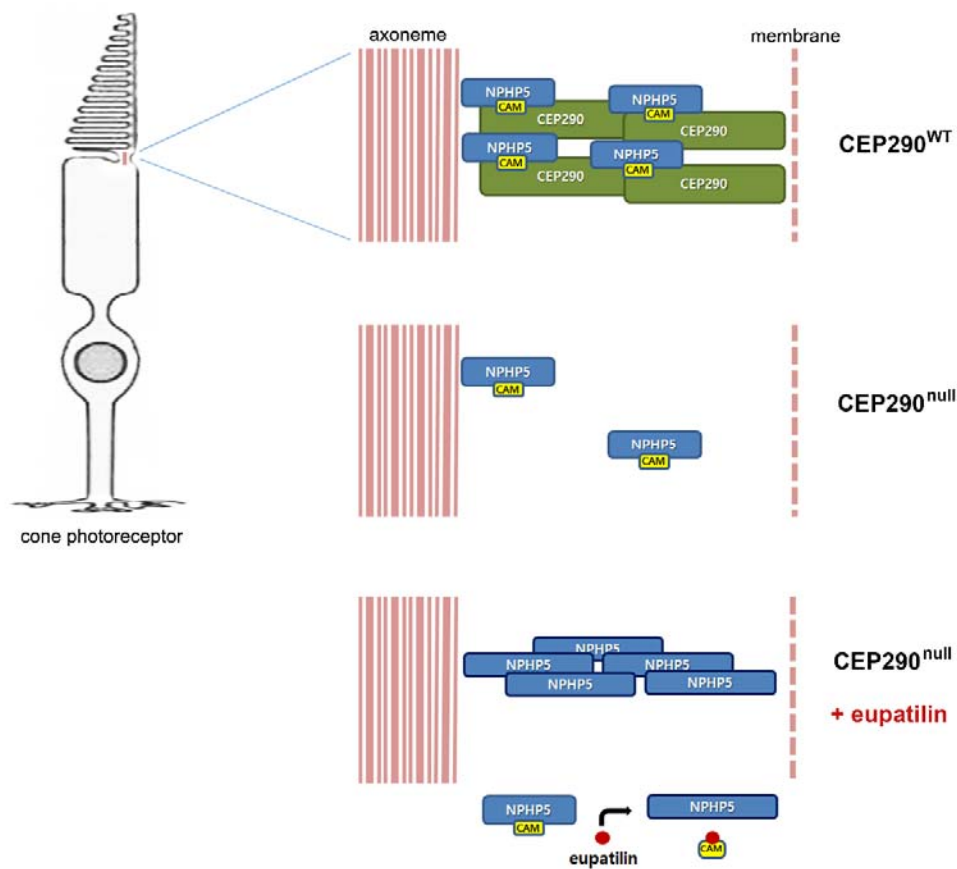
Supplemental Figure 10. Recruitment of TCTN1 and TMEM216 to the ciliary transition zone in CEP290^{null} RPE1-Smo-EGFP cells. (A) Immunofluorescence micrographs visualizing TCTN1 in CEP290^{WT} and CEP290^{null} RPE1-Smo-EGFP cells after serum starvation for 24 h. Anti-glu-TUB antibody labels the centriole/basal body and the ciliary axoneme. (B) Immunofluorescence micrographs visualizing TMEM216 in CEP290^{WT} and CEP290^{null} RPE1-Smo-EGFP cells after serum starvation for 24 h. Scale bars indicate 5 μ m.



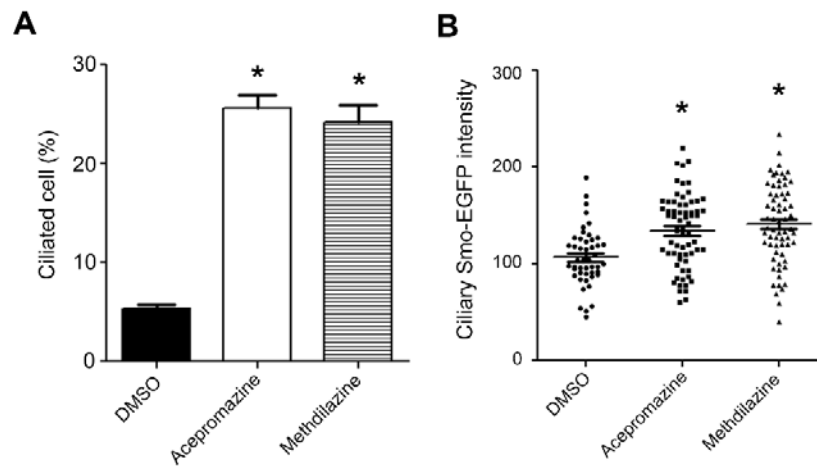
Supplemental Figure 11. Effect of eupatilin on ciliogenesis in NPHP5-depleted CEP290^{null} RPE1-Smo-EGFP cells. (A) Immunoblotting for the indicated proteins after transfection of control and NPHP5 shRNAs. (B) Effect of eupatilin on serum starvation-induced ciliogenesis in CEP290^{null} RPE1-Smo-EGFP cells transfected with the indicated shRNAs. Anti-ARL13B antibody was used as a cilium marker. Error bars represent SEM (n = 3 independent experiments; *P<0.05, t-test).



Supplemental Figure 12. Molecular docking analysis of human calmodulin with eupatilin using the CDOCKER algorithm. The result of 3-dimensional molecular docking analysis on human calmodulin (Protein Data Bank code 1CTR) with eupatilin (PubChem CID 5273755) was performed by discovery studio 2016 software. In the virtual docking model of calmodulin, an oxygen atom of eupatilin residue forms a hydrogen bond with Glu 11 in the hydrophobic pocket of calmodulin. In addition, Glu 127 and Met 144 of calmodulin form Pi-Anion and Pi-Sulfur interaction, respectively, resulting in a high affinity and direct interaction with eupatilin. The best CDOCKER energy between human calmodulin and eupatilin was -13.5633 kcal/mol. The 2-dimensional diagram shows the interaction between key residues and eupatilin.



Supplemental Figure 13. A model for eupatilin-mediated rescue of transition zone function in CEP290^{null} cells. Calmodulin-bound NPHP5 is associated with CEP290 at the transition zone. In CEP290^{null} background, calmodulin-bound NPHP5 is not efficiently recruited to the transition zone. Eupatilin-mediated inhibition of calmodulin binding to NPHP5 promotes the recruitment and accumulation of NPHP5 at the transition zone. Elevated NPHP5 levels or functions may compensate for the loss of CEP290.



Supplemental Figure 14. Acepromazine and methdilazine rescue ciliary defects in CEP290^{null} RPE1-Smo-EGFP cells. (A) Effect of acepromazine and methdilazine on ciliogenesis in CEP290^{null} RPE1-Smo-EGFP cells. **(B)** Quantification (arbitrary unit) of the ciliary Smo-EGFP intensity after acepromazine and methdilazine treatment. Error bars represent SEM (>50 cells of each condition from two independent experiments were analyzed; * P<0.05, t-test).